NANO LETTERS

pubs.acs.org/NanoLett Letter

Mapping the Magnetic Field Intensity of Light with the Nonlinear Optical Emission of a Silicon Nanoparticle

Guang-Can Li, Jin Xiang, Yong-Liang Zhang, Fu Deng, Mingcheng Panmai, Weijie Zhuang, Sheng Lan,* and Dangyuan Lei*

Cite This: *Nano Lett.* 2021, 21, 2453−2460 Read Online

ACCESS | Metrics & More | Article Recommendations | Supporting Information

ABSTRACT: To detect the magnetic component of arbitrary unknown optical fields, a candidate probe must meet a list of demanding requirements, including a spatially isotropic magnetic response, suppressed electric effect, and wide operating bandwidth. Here, we show that a silicon nanoparticle satisfies all these requirements, and its optical magnetism driven multiphoton luminescence enables direct mapping of the magnetic field intensity distribution of a tightly focused femtosecond laser beam with varied polarization orientation and spatially overlapped electric and magnetic components. Our work establishes a powerful nonlinear optics paradigm for probing unknown optical magnetic fields of arbitrary electromagnetic structures, which is not only essential for realizing subwavelength-scale optical magnetometry but also facilitates nanophotonic research in the magnetic light−matter interaction regime.

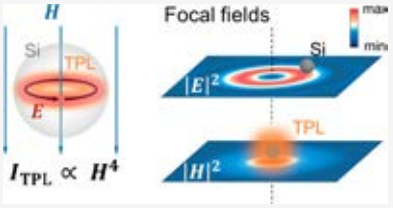

KEYWORDS: *magnetic nanoprobe, optical magnetism, silicon nanoparticle, Mie resonance, multiphoton photoluminescence*

To boost light−matter interactions in nanomaterials/nanostructures (for example, plasmonic nanoparticles,[1] quantum dots,[2] etc.), tightly confined optical fields, such as highly focused light beams[3] or bounded surface waves,[4,5] are frequently employed as excitation sources. Due to the diffraction-limited confinement dimensions, nanometric objects immersed in such complex fields often exhibit strong position-dependent optical responses.[6,7] For this reason, the exact knowledge of the excitation field profile is crucial for leveraging the light−matter interaction in nanoscale optics. While the techniques for mapping the electric field of light have been well-established,[8] solutions addressing its magnetic counterpart remain far from satisfactory, due mainly to the lack of an effective magnetic field probe working at optical frequencies.

In the past decade, several nanoscale paradigms have been used to probe the magnetic field of light, such as rare earth ions (REIs), split ring resonators (SRRs), and ring-shaped plasmonic nanoantennas. These magnetic probes have been either integrated to near-field scanning tips to probe the surface magnetic fields[4,5] or directly utilized to map the magnetic field distribution profiles of tightly focused laser beams.[9] Nevertheless, three functionality limitations impede universal applications of these linear optical probes, including (1) magnetic monopole-like response, (2) significant electric-magnetic crosstalk, and (3) limited working frequencies. For instance, the first demonstrated magnetic field probe working at optical frequencies is based on the SRR nanoconstruct that solely responds to the magnetic field component perpendicular to the SSR plane.[4] In addition, the metal-based magnetic probes suffer from unavoidable Ohmic losses at optical frequencies, for which the magnetic responses are typically weak and mostly observable in the near-infrared spectral range.[1,4,10,11] On the other hand, a single REI can only sense the magnetic field component aligned with its magnetic transition dipole moment.[12] Although REIs can be heavily doped into a dielectric nanoparticle to generate a spatially averaged magnetic response,[13] the required ultrahigh doping concentration imposes a significant challenge on sample fabrication. Besides, the small spectral separation between the electric and magnetic transition frequencies (typically <10 nm) in the REIs induces a significant electric-magnetic crosstalk,[9] which would easily smear the mapped field profiles. Similar concerns also appear for metal SSRs and ring-shaped plasmonic nanoprobes, of which the magnetic resonances are usually mixed with their broadband electric counterparts.[1,14,15] Finally, the naturally occurring candidates such as REIs can exhibit magnetic responses in the visible light spectrum, but the available working frequencies are limited by their spectrally discrete magnetic dipole transitions.[16]

Magnetic field distribution can also be retrieved from known electric field distribution via Maxwell's curl equation, i.e., $\nabla \times E = -\frac{\partial B}{\partial t}$. While this strategy relaxes the demanding requirement of a magnetic field probe with a dominant electric

Received: November 28, 2020
Revised: February 25, 2021
Published: March 2, 2021

https://dx.doi.org/10.1021/acs.nanolett.0c04706
Nano Lett. 2021, 21, 2453−2460

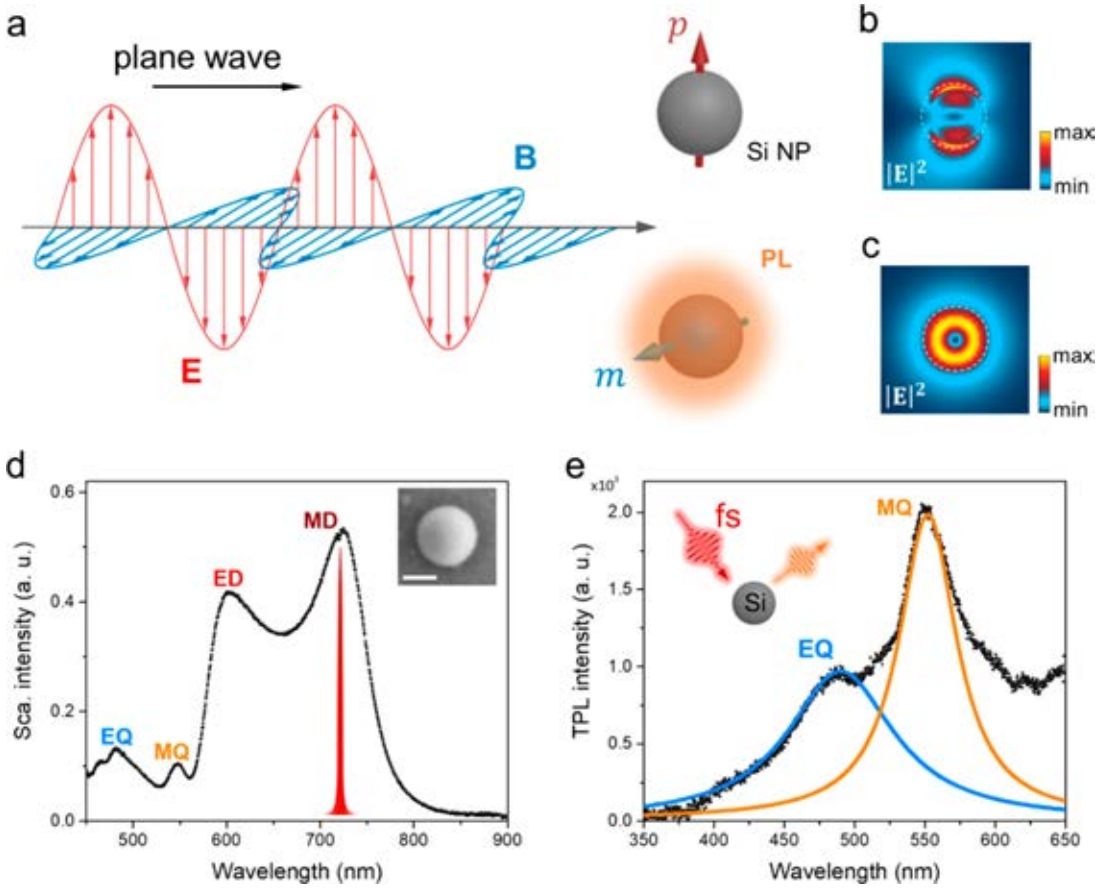

Figure 1. Optical magnetism driven MPL from single Si nanoparticles. (a) Schematic illustration of a Si nanoparticle (Si NP) responding selectively to the electric (upper panel) or magnetic (lower panel) field component of a plane wave. p (m) denotes the electric (magnetic) dipole moment induced by the incident light. (b, c) Normalized near-field intensity distribution profiles for a Si nanoparticle, with exclusive excitation of its ED (b) or MD (c) resonance mode by vector optical fields (for more details see Supporting Information Section 1). Here the Si nanoparticle is 185 nm in diameter, and the excitation wavelength is set to match its MD resonance at 720 nm (see Methods). (d) Measured scattering spectrum of a silica-supported Si nanoparticle with a diameter of ~180 nm, with the inset showing its scanning electron microscopy (SEM) micrograph. Scale bar in the inset, 100 nm. (e) Two-photon luminescence spectrum of the Si nanoparticle in (d), measured upon excitation of the MD resonance by a tightly focused femtosecond laser beam. The data is fitted with double singlet-Lorentz functions (colored) to distinguish the multipole emission modes.

response, the electric field distribution has to be measured with sufficient high spatial precision in three-dimensional space. Besides, the retrieve methods typically rely on complicated measurement setups such as near-field scanning optical microscopy (NSOM)[17] and photoemission electron microscopy (PEM),[18] with the latter only applicable to optical fields near the metal surface.

In this letter, we demonstrate a simple and straightforward method to exclusively map the magnetic field intensity distribution of light with single spherical silicon (Si) nanoparticles. Such a Si nanoprobe has been recently used to probe the magnetic[19] and longitudinal transverse density of light,[20] but the employed far-field scattering based method can only resolve the longitudinal magnetic field component (i.e., H_z) or magnetic fields exhibiting spinning vector characters. Here we exploit the nonlinear optical emission properties of single Si nanoparticles, and show that such a nonlinear magnetic nanoprobe enables direct mapping of the intensity distributions of unknown magnetic fields with arbitrary electromagnetic structures thanks to its unique merits. It has (1) a spatially isotropic magnetic response endowed by spherical symmetry, (2) a negligible crosstalk between the electric and magnetic responses ensured by both substantial spectral and spatial separations, (3) a far-field multiphoton luminescence (MPL) exclusively driven by the magnetic component of light, and (4) a tunable magnetic dipolar resonance across the whole visible and near-infrared spectral range.

RESULTS AND DISCUSSION

The physical mechanism for probing optical magnetic fields with the proposed nonlinear nanoprobes can be understood by the scenario of a single silicon nanoparticle interacting with a plane wave (Figure 1a). Based on Mie theory, a single Si nanoparticle with an appropriate size supports strong electric dipole (ED) and magnetic dipole (MD) resonances, and weak electric quadrupole (EQ) and magnetic quadrupole (MQ) resonances, all in the visible to near-infrared spectral range (Figure 1d),[21,22] which allows it to respond selectively to the electric or magnetic field of the incident light via either the ED or MD excitation. In particular, resonant excitation of the MD resonance generates strong electric field confined mainly inside the nanoparticle (Figure 1c), which can be exploited to boost efficiently the nonlinear optical response[23] like MPL.[24,25] Such optical magnetism driven nonlinear emission thus renders the Si nanoparticle a local field sensor enabling far-field detection of the magnetic component of light, in the same way as that

https://dx.doi.org/10.1021/acs.nanolett.0c04706
Nano Lett. 2021, 21, 2453−2460

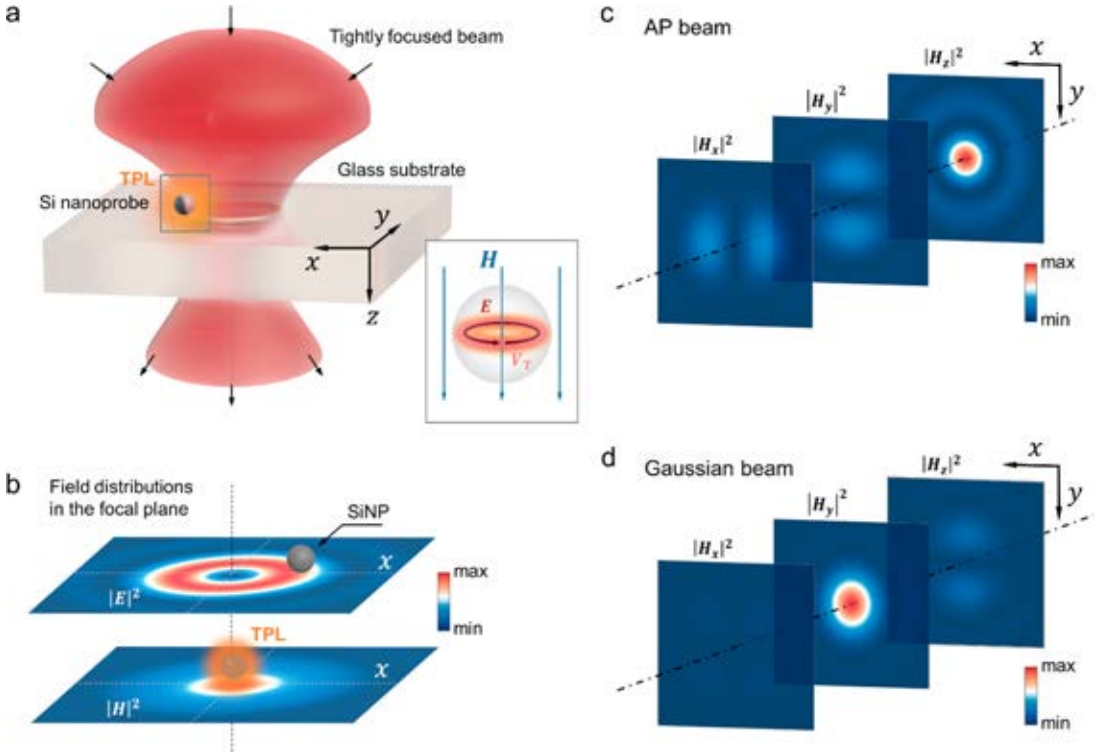

Figure 2. Principle for mapping the magnetic field of a tightly focused light beam using a single Si nanoparticle. (a) A silica-supported Si nanoparticle is raster scanned through the focal plane of a tightly focused light beam. The position-dependent photoluminescence signal emitted from the nanoparticle is recorded, forming a scanning image recording the intensity distribution of the driving field component. The inset depicts that the inner-particle electric field (E), induced by an external magnetic field (H), is concentrated mainly near the equatorial plane, forming a torque-shaped domain (V_T) (see the simulated three-dimensional field distribution pattern in Figure S2). (b) The Si nanoparticle is lightened up at the position where the magnetic field is nonvanishing. The stacked planes depict the focal electric (upper) and magnetic (lower) field distributions of an azimuthally polarized (AP) beam. (c, d) Intensity distributions of the magnetic field component of an AP (c) and a linearly polarized Gaussian beam (d) in the focal plane. The Gaussian beam is x-polarized before being focused. The numerical aperture (NA) of the focusing lens is 0.95, and the wavelength of the incident beam is 720 nm, consistent with the experimental conditions used in (a). The stacked images in each figure are rendered on the same intensity scale.

using single fluorescent molecules[26] or metal nanoparticles[3] to probe the electric field of light.

Owing to the indirect bandgap, bulk Si is known to be a semiconductor material notorious for its extremely low photoluminescence quantum efficiency (10^{-7}). Nevertheless, nanostructured Si can emit strong luminescence upon delicate excitation of the appropriate Mie resonances.[24] Figure 1e displays the typical luminescence response of a Si nanoparticle excited at the MD resonance. Within the emission band of interest, the luminescence spectrum exhibits two pronounced intensity maxima at the MQ and EQ resonances, indicating enhanced spontaneous emission through the Purcell effect.[27] Since Si is a nonmagnetic material at optical frequencies, the photoluminescence emitted from the Si nanoparticles must originate from the electronic transitions driven by the inner-particle electric fields. Figure 1b,c show that, at the MD resonance, the excitation consists of both ED and MD components that jointly contribute to the generation of the particle-confined electric fields. However, the ED-related near-field distribution exhibits a poor spatial overlapping with the nanoparticle volume, rendering the MPL from the Si nanoparticle dominantly contributed by the MD excitation (see Supporting Information Section 1). In addition, the large spectral separation (typically >100 nm, refer to Figure 1d) between the MD and ED resonances can further reduce the electric-magnetic crosstalk in either excitation process. Such concurrent spatial and spectral exclusion of the ED component at the MD resonance thus leads to a cooperative suppression of the electric contribution to the total MPL, rendering the single Si nanoparticle an artificial magnetic emitter responding solely to the magnetic field of light.

Following the above rationale, a semianalytical model is developed to relate qualitatively the measured photoluminescence from a single Si nanoparticle to the external driving magnetic field. Within the quasi-static approximation, the Si nanoparticle at the MD resonance acts as a magnetic dipole responding linearly to the external magnetic field, written as

$$\vec{m} = \alpha_m \vec{H}_0(\vec{r}) \tag{1}$$

where $\vec{m}$ is the magnetic dipole moment, α_m is the magnetic dipole polarizability, and $\vec{H}_0$ is the external magnetic field at position $\vec{r}$. This dipolar magnetic response essentially originates from the structured polarization in the nanoparticle. Considering the relatively small size parameter ($2a/\lambda \sim 0.5$) of a silicon nanoparticle at the wavelength of the MD resonance,[28,29] its structural magnetic dipole moment can be evaluated with the long-wave approximation, *i.e.*,

$$\vec{m} = -\frac{i\omega_0}{2}\int_V \vec{r'} \times \vec{P'}(\vec{r'})\,\mathrm{d}V$$
$$\text{with } \vec{P'}(\vec{r'}) = (\epsilon_s - \epsilon_0)\vec{E'}(\vec{r'}) \tag{2}$$

https://dx.doi.org/10.1021/acs.nanolett.0c04706
Nano Lett. 2021, 21, 2453−2460

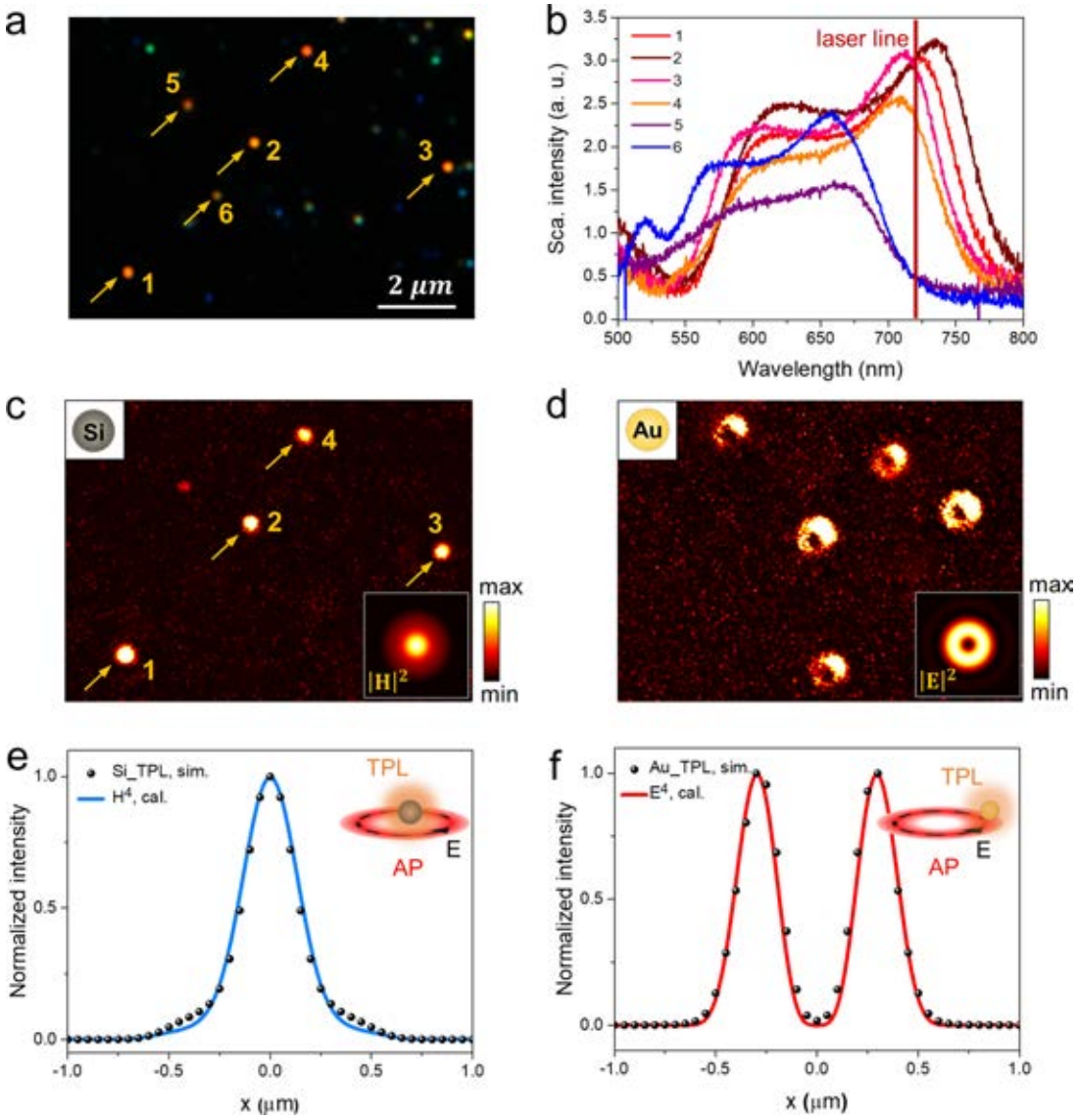

Figure 3. Mapping the magnetic (electric) field intensity distribution of an AP beam with single Si (Au) nanoparticles. (a) Dark-field microscope image of a sample area of interest. The bright red spots (labeled as 1, 2, 3, and 4) are Si nanoparticles having MD resonances at ∼720 nm, while the other ones, dimmer or vivid green, correspond to smaller Si nanoparticles with MD resonances at shorter wavelengths. (b) Scattering spectra measured for the Si nanoparticles marked in (a). (c) TPL image obtained by scanning the Si nanoparticles across the focal plane of a focused AP beam. The inset shows the calculated magnetic field distribution in the focal plane, with the same objective and laser parameters as used in experiments. (d) TPL image obtained by scanning Au nanoparticles (characterization details in Supporting Information Section 5) through the focal plane of the same AP beam as in (c). The nominal diameter of the nanoparticles is ∼100 nm. Their plasmon responses are featured by a prominent resonance at ∼550 nm (see the measured scattering spectra in Figure S6d). Inset shows the calculated electric field distribution in the focal plane. (e) Position-dependent TPL excitation efficiency simulated for a Si nanoparticle (diameter, 185 nm) scanned across the focal plane of an AP beam, with the data sampled along the radial direction (black dots). The calculated $|H|^4$ in the focal plane is also provided for comparison (blue curve). (f) Similar results as (c) but for a Au nanoparticle (diameter, 100 nm).

where ω_0 is the angular frequency of the excitation, V is the nanoparticle volume, $\vec{r'}$ is position vector defined in the local coordinate frame attached to the nanoparticle, $\vec{P'}$ represents the local polarization, ϵ_s (ϵ_0) is the permittivity of Si (vacuum), and $\vec{E'}(\vec{r'})$ specifies the local electric field inside the nanoparticle. At the MD resonance, the inner-particle electric fields are confined mainly in the torque-shaped volume (V_T) near the equatorial plane (see inset of Figure 2a, colored in red), indicating a highly localized source for both the far-field MD response and the photoluminescence (refer to eq S3 in Supporting Information Section 2). In this regard, the torque-shaped volume V_T can be assigned as the effective integrating domain for the integration term in eq 2. Within the scalar approximation (for details see Supporting Information Section 2), combining eqs 1 and 2 leads to

$$
\begin{aligned}
&-\frac{i\omega_0(\epsilon_s-\epsilon_0)}{2}\int_V \vec{r'}\times\vec{E'}(\vec{r'})\,\mathrm{d}V \\
&=\alpha_m\vec{H}_0(\vec{r}) \\
&\approx -\frac{i\omega_0(\epsilon_s-\epsilon_0)}{2}V_T\langle|\vec{E'}|\rangle\vec{e}
\end{aligned}
\tag{3}
$$

https://dx.doi.org/10.1021/acs.nanolett.0c04706
Nano Lett. 2021, 21, 2453−2460

where $\langle|\vec{E'}|\rangle$ is the averaged magnitude of the electric field in V_T, *i.e.*, $\langle|\vec{E'}|\rangle = \frac{1}{V_T}\int_{V_T}|\vec{E'}|\,dV$. $\vec{e}$ specifies the unit vector parallel to $\vec{H}_0$. In a phenomenological approach, the photoluminescence from the Si nanoparticle can be evaluated by[30,31]

$$I_{PL}(\vec{r},\omega) \propto \int_V |\vec{E'}(\vec{r'})|^{2n}\sigma^{(n)}_{\omega_0}\rho_{\omega_0,\omega}\gamma_\omega\,dV \tag{4}$$

where $\sigma^{(n)}$ specifies the photon absorption probability at the excitation frequency ω_0, with n denoting the kind of absorption, ω is the emission frequency, and ρ and γ represent the thermalization and emission probabilities, respectively, which are position independent. Throughout this study, the excitation wavelength was chosen at ∼720 nm, and the photoluminescence from the Si nanoparticle was dominated by two-photon absorption (n = 2) induced luminescence (TPL) (see details in the Supporting Information Section 3). In this case, eq 4 can be reduced and approximated to the following form:

$$I_{TPL}(\vec{r}) \propto \int_V |\vec{E'}(\vec{r'})|^{2n}\sigma^{(n)}_{\omega_0}\rho_{\omega_0,\omega}\gamma_\omega\,dV \tag{5}$$

where $\langle|\vec{E'}|^4\rangle$ is the averaged magnitude of $|\vec{E'}|^4$ in V_T, *i.e.*, $\langle|\vec{E'}|^4\rangle = \frac{1}{V_T}\int_{V_T}|\vec{E'}|^4\,dV$. We assume $|\vec{E'}|$ varies slowly in V_T and, thus, have $\langle|\vec{E'}|^4\rangle \approx \langle|\vec{E'}|\rangle^4$. With this approximation, combining eq 3 and 5 leads to

$$I_{TPL}(\vec{r}) \propto |\vec{H}_0(\vec{r})|^4 \tag{6}$$

This representation explicitly relates the external magnetic field with the TPL intensity of the Si nanoparticle, thereby allowing mapping the magnetic field distribution profile by measuring the far-field TPL intensity.

To demonstrate the above-proposed approach of using Si nanoparticles as magnetic field nanoprobes, we chose tightly focused laser beams as the testing optical fields. As illustrated in Figure 2a, a silica-supported Si nanoparticle is raster scanned through the focal plane, and the emitted TPL within the MQ emission band (∼530−570 nm) is collected. The formed image would thus record either the electric or the magnetic field intensity distribution in the focal plane, depending on whether the nanoprobe responds to the electric or the magnetic field of the focused light beam.

We first chose an azimuthally polarized (AP) laser beam to examine the effectiveness of the proposed magnetic field nanoprobe. As shown in Figure 2b, the electric field distribution in the focal plane of the beam displays a doughnut-shaped pattern, with an intensity null on the optical axis (calculated via the vectorial diffraction theory[32]). The magnetic field distribution, however, forms a circular spot, with the peak intensity on the optical axis. Such spatially separated electric and magnetic field distributions are suited for clarifying whether the nanoprobe responds to the electric or the magnetic field of the focused laser beam.[9] In our experiment, Si nanoparticles were fabricated with the femtosecond laser ablation method,[24] which produced nearly spherical particles randomly dispersed on a silica substrate. We intentionally selected a large area containing several well-separated Si nanoparticles (Figure 3a), some having an MD resonance close to the 720 nm laser wavelength (hereinafter referred to as "MD nanoparticles", Figure 3b). Figure 3c displays the image obtained by raster scanning this sample area through the focal plane of the AP beam of the same wavelength. In sharp contrast to the dark-field image shown in Figure 3a, only the MD nanoparticles are efficiently lightened in the TPL image, while the off-resonant Si nanoparticles are barely observable. Moreover, each MD nanoparticle appears as a circular bright spot, consistent with the intensity distribution of the magnetic field in the focal plane of the focused AP beam (see inset in Figure 3c). This coincidence verifies that the TPL signals of these MD nanoparticles are dominantly driven by the magnetic field of the incident light. It is also noticed that the sizes of the bright spots appear to be slightly different, although they image the same focal field of the AP beam. This phenomenon, as revealed by simulation results, is mainly caused by different TPL excitation efficiencies of the Si nanoparticles: the closer of the MD resonance of a Si nanoparticle to the laser wavelength, the higher its excitation efficiency and thus the larger the intensity of the retrieved TPL pattern (see details in Supporting Information Section 4).

For comparison, we replaced the Si nanoprobes with spherical Au nanoparticles (average diameter, ∼100 nm). These Au nanoparticles exhibit dominant electric responses at the laser wavelength and thus can be exploited to probe the electric field of light. Figure 3d shows the image obtained by scanning a few Au nanoparticles through the same beam focus used in Figure 3c, with the map intensity rendered by the TPL of Au (emission band, ∼500−600 nm). As expected, the luminescence maps of single Au nanoparticles well reproduce the doughnut-shaped electric field distribution of the focused AP beam (see the bottom-right inset in Figure 3d).

In a phenomenological way, the above experimental results can be numerically simulated via inspecting the position-dependent TPL excitation efficiency of a Si nanoparticle. This can be performed by calculating the integral in eq 5 over the volume of a Si nanoparticle scanning through the focus of an AP beam, with the electric fields extracted from electromagnetic simulation results (see Methods). Figure 3e,f shows the TPL excitation efficiencies simulated for a Si nanoparticle and a Au nanoparticle, respectively, both sampled along the radial direction of the beam focus. It is found that the excitation efficiency profile in Figure 3e well reproduces the TPL pattern of the Si nanoparticle revealed in the raster-scanned TPL image shown in Figure 3c and also agrees well with that of the magnetic field distribution in the focal plane (inset in Figure 3c). Such agreement is also found between the TPL pattern of the Au nanoparticle (Figure 3d) and the simulated excitation efficiency profile (Figure 3f) or the calculated electric field distribution in the focal plane (inset in Figure 3d). In particular, the spatially varying excitation efficiency of the single Si nanoprobe perfectly follows the calculated position-dependent $|H|^4$, in consistence with the prediction by our semianalytical model (eqs 1−6).

For the focused AP beam, the magnetic field in the focal plane is dominated by the longitudinal component parallel to the beam axis (H_z, Figure 2c). In order to demonstrate that Si nanoparticles are capable of probing magnetic fields with arbitrary polarization orientations, we subsequently replaced the AP beam with a Gaussian beam. In contrast to the AP beam, the focal magnetic field of the Gaussian beam is dominated by the transverse component (for example, H_y, see Figure 2d), which is not readily accessible to the metal rings[14] or SSR-based probes.[4] Complicating matters, the transverse magnetic field of a focused Gaussian beam spatially overlaps with its electric counterpart (see insets in Figure 4a,b) and,

https://dx.doi.org/10.1021/acs.nanolett.0c04706
Nano Lett. 2021, 21, 2453−2460

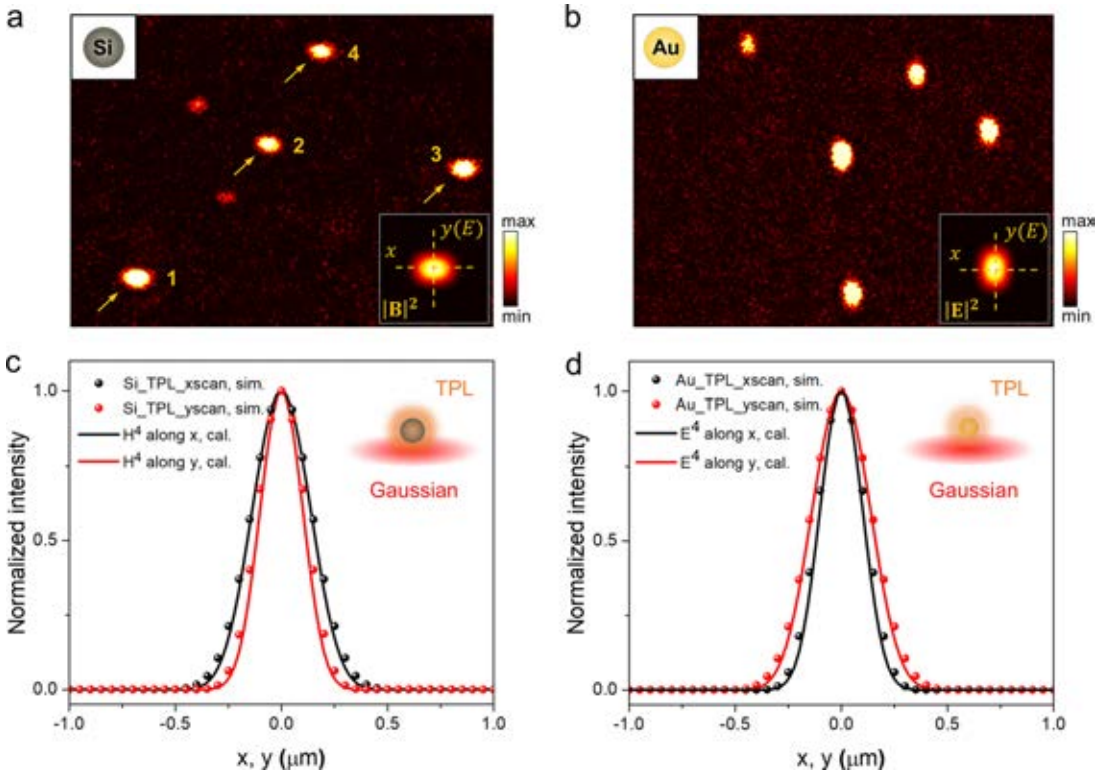

Figure 4. Mapping the magnetic (electric) field intensity distribution of a linearly polarized Gaussian beam with single Si (Au) nanoparticles. (a) TPL images of individual Si nanoparticles obtained by scanning the sample area in Figure 3a through the focal plane of a focused Gaussian beam. The Gaussian beam is *y*-polarized before being focused by the objective. (b) TPL images of individual Au nanoparticles obtained by scanning the sample area in Figure 3d through the same focused beam used in (a). (c) Position-dependent TPL excitation efficiency simulated for a Si nanoparticle (diameter, 185 nm) scanned along the radial direction (*x* or *y*) of a focused Gaussian beam. The calculated $|H|^4$ profile of the focused Gaussian beam along the *x* or *y* axis is also provided for comparison. (d) Similar results as (c) but for a Au nanoparticle (diameter, 100 nm).

therefore, cannot be resolved with probes exhibiting simultaneous electric and magnetic responses. With the same Si and Au nanoparticles (as employed in Figure 3) scanning through the focus of a Gaussian beam, we obtain the mapping results shown in Figure 4a,b, where both types of nanoparticles appear as elliptical bright spots, in sharp contrast to the circular bright spots or the doughnut-shaped patterns observed for the AP beam (Figure 3). However, the long axes of the elliptical spots for the Au nanoparticles are parallel to the input laser polarization while those for the Si nanoparticles are perpendicular to it. Such asymmetric patterns are also observed in the calculated magnetic and electric field distributions in the focal plane (insets in Figure 4a,b), implying that the single Si (Au) nanoparticles are capable of imaging the magnetic (electric) component of the excitation field. Nevertheless, the magnetic field distributions mapped by single Si nanoparticles may be affected by the accompanying electric field due to the spatial overlapping of the electric and magnetic fields in the focal plane. Such a crosstalk effect can be evaluated by inspecting the TPL excitation efficiency of a Si nanoparticle scanned through the focused Gaussian beam. As shown in Figure 4c, we observe no significant deviation between the simulated TPL excitation efficiency and the calculated $|H|^4$ profile in the focal plane, suggesting a negligible electric−magnetic crosstalk effect. In other words, the single Si nanoparticles exclusively map the magnetic component of the focused Gaussian beam, with no smearing by the accompanying electric component. Conversely, the TPL excitation efficiency of a Au nanoparticle perfectly follows the $|E|^4$ profile of the focal fields (Figure 4d), in line with the fact that single plasmonic nanoparticles are mainly electric-field responsive.

It should be emphasized that we employed the MPL instead of coherent nonlinear emissions (for example, second-harmonic generation[33,34]) to map the magnetic fields of focused laser beams. This is because MPL is essentially a spontaneous emission process insensitive to the polarization state of excitation fields. Such an incoherent character enables uniform emission characteristics (angular distribution, emission polarization, *etc.*) of the MPL from spherical Si nanoprobes, which is essential for mapping unknown fields, especially the ones with concurrent multiple magnetic components (one demonstration provided in Supporting Information Section 6). In addition, the distinct electric field distributions at the ED and MD resonances ensure negligible contribution of the ED excitation to the MPL of the Si nanoparticle, which is not available when the coherent nonlinear optical processes (e.g., harmonic generation) are employed. Also, it is important to note that a scattering based nanointerferometric scheme demonstrated by Bauer et al.,[3] initially used to map the electric field distributions of tightly focused laser beams, could be generalized to probe the magnetic field component by simply replacing the plasmonic nanoparticle with a Si one. The only concern is the possible electric−magnetic crosstalk in the far-field scattering signals,[35] as manifested in the spectral overlap between the ED and the MD resonances (refer to Figure 1d). A recent study reported that a Au-core−Si-shell nanoparticle can exhibit an ideal

https://dx.doi.org/10.1021/acs.nanolett.0c04706
Nano Lett. 2021, 21, 2453−2460

magnetic dipole scattering response by elegantly overlapping the MD and anapole resonances.[36] However, such a pure MD character was only observed in the far-field scattering response and not excited exclusively by the magnetic field of external light. Another key advantage of the Si nanoprobes is that their magnetic resonances can be spectrally tuned by simply controlling the particle size, which renders a wide operating wavelength (see Supporting Information Section 7).

In summary, we have demonstrated a novel nanoprobe for detecting the magnetic component of light fields with arbitrary electromagnetic structures. This probe is based on a spherical Si nanoparticle with an efficient MPL driven exclusively by the magnetic field component of light. Using such Si nanoprobes, we have successfully mapped the magnetic field intensity distributions of two representative femtosecond laser beams tightly focused by a high numerical aperture objective: an AP vector beam featuring a dominant longitudinal magnetic component and a linearly polarized Gaussian beam showing a dominant transverse magnetic component. The probing mechanism presented here is also applicable to other high-index semiconductor nanoparticles showing significant structural magnetic resonances, namely, Ge or GaAs nanoparticles.[37] The detection of focused continuous wave laser beams will be possible by using semiconductor nanoparticles with direct bandgaps which emit single-photon luminescence.[38] Looking forward, we anticipate that a more advanced probing scheme can be developed by attaching Si nanoparticles to near-field scanning tips, with which the magnetic near-fields bound to a waveguide surface or plasmonic nanostructures can be revealed.

METHODS

Experimental Setup. Details are provided in Supporting Information Section 8.

Numerical Simulations. The electromagnetic response of a single Si nanoparticle was simulated by the three-dimensional finite-difference time-domain (FDTD) method implemented on a commercial electrodynamic simulation package (FDTD Solutions, Lumerical Inc.). For simplicity, the nanoparticle is immersed in air. The exclusion of the silica substrate present in the experiment does not significantly modify the resonance characteristics of Si nanoparticles and disable the Si nanoprobe for exclusively mapping the magnetic field intensity of light (for details see Supporting Information Section 9). The dielectric constant of Si is extrapolated from the Palik experimental data.[39] The Si nanoparticle is illuminated either with a plane wave to resolve its Mie-type multipole resonances or with focused light beams to mimic the experimental excitation conditions. To ensure the iteration convergence, a mesh size of 1 nm is used within the nanoparticle volume.

ASSOCIATED CONTENT

Supporting Information

The Supporting Information is available free of charge at https://pubs.acs.org/doi/10.1021/acs.nanolett.0c04706.

Experimental setup, characterization of the linear and nonlinear optical responses of gold nanoparticles, evaluation of substrate effects, details of the approximation made in the main text, and extended numerical investigations of silicon nanoprobes (PDF)

AUTHOR INFORMATION

Corresponding Authors

Sheng Lan − *Guangdong Provincial Key Laboratory of Nanophotonic Functional Materials and Devices, School of Information and Optoelectronic Science and Engineering, South China Normal University, Guangzhou 510006, China*; Email: slan@scnu.edu.cn

Dangyuan Lei − *Department of Materials Science and Engineering, City University of Hong Kong, Kowloon, Hong Kong SAR*; orcid.org/0000-0002-8963-0193; Email: dangylei@cityu.edu.hk

Authors

Guang-Can Li − *Guangdong Provincial Key Laboratory of Nanophotonic Functional Materials and Devices, School of Information and Optoelectronic Science and Engineering, South China Normal University, Guangzhou 510006, China; Department of Materials Science and Engineering, City University of Hong Kong, Kowloon, Hong Kong SAR*; orcid.org/0000-0002-9903-8900

Jin Xiang − *Guangdong Provincial Key Laboratory of Nanophotonic Functional Materials and Devices, School of Information and Optoelectronic Science and Engineering, South China Normal University, Guangzhou 510006, China*

Yong-Liang Zhang − *State Key Laboratory of Superlattices and Microstructures, Institute of Semiconductors, Chinese Academy of Sciences, Beijing 100083, China*

Fu Deng − *Guangdong Provincial Key Laboratory of Nanophotonic Functional Materials and Devices, School of Information and Optoelectronic Science and Engineering, South China Normal University, Guangzhou 510006, China*

Mingcheng Panmai − *Guangdong Provincial Key Laboratory of Nanophotonic Functional Materials and Devices, School of Information and Optoelectronic Science and Engineering, South China Normal University, Guangzhou 510006, China*

Weijie Zhuang − *Guangdong Provincial Key Laboratory of Nanophotonic Functional Materials and Devices, School of Information and Optoelectronic Science and Engineering, South China Normal University, Guangzhou 510006, China*

Complete contact information is available at: https://pubs.acs.org/10.1021/acs.nanolett.0c04706

Author Contributions

G.-C.L., S.L., and D.Y.L. conceived the idea. G.-C.L., J.X., and W.-J.Z. carried out the experimental work. G.-C.L. performed the calculations with the help of Y.-L.Z., D.F., and M.P. G.-C.L. drafted the manuscript with inputs from all the authors. S.L. and D.Y.L. cosupervised the project and revised the manuscript.

Funding

This work was supported by the National Key Research and Development Program of China (No. 2016YFA0201002), the National Natural and Science Foundation of China (Grant Nos. 11674110, 11874020, and 11904110), the Natural Science Foundation of Guangdong Province, China (Grant No. 2016A030308010), China Postdoctoral Science Foundation (Grant No. 2019M652930), the Startup Foundation of Institute of Semiconductors, Chinese Academy of Sciences (No. E0SEBB01), and the Research Grants Council of Hong Kong (GRF Grant No. 15303417).

Notes

The authors declare no competing financial interest.

https://dx.doi.org/10.1021/acs.nanolett.0c04706
Nano Lett. 2021, 21, 2453−2460

■ ACKNOWLEDGMENTS

We appreciate the useful discussions with Prof. Yuri Kivshar and Prof. Anatoly Zayats.

■ REFERENCES

(1) Fan, J. A.; Wu, C.; Bao, K.; Bao, J.; Bardhan, R.; Halas, N. J.; Manoharan, V. N.; Nordlander, P.; Shvets, G.; Capasso, F. Self-Assembled Plasmonic Nanoparticle Clusters. *Science* **2010**, *328* (5982), 1135−1138.
(2) Ribeiro, H.; Burkard, G. Join the Dots. *Nat. Mater.* **2013**, *12* (6), 467−467.
(3) Bauer, T.; Orlov, S.; Peschel, U.; Banzer, P.; Leuchs, G. Nanointerferometric Amplitude and Phase Reconstruction of Tightly Focused Vector Beams. *Nat. Photonics* **2014**, *8* (1), 23−27.
(4) Burresi, M.; van Oosten, D.; Kampfrath, T.; Schoenmaker, H.; Heideman, R.; Leinse, A.; Kuipers, L. Probing the Magnetic Field of Light at Optical Frequencies. *Science* **2009**, *326* (5952), 550−553.
(5) le Feber, B.; Rotenberg, N.; Beggs, D. M.; Kuipers, L. Simultaneous Measurement of Nanoscale Electric and Magnetic Optical Fields. *Nat. Photonics* **2014**, *8* (1), 43−46.
(6) Neugebauer, M.; Woźniak, P.; Bag, A.; Leuchs, G.; Banzer, P. Polarization-Controlled Directional Scattering for Nanoscopic Position Sensing. *Nat. Commun.* **2016**, *7* (1), 11286.
(7) Woźniak, P.; Banzer, P.; Leuchs, G. Selective Switching of Individual Multipole Resonances in Single Dielectric Nanoparticles. *Laser Photon. Rev.* **2015**, *9* (2), 231−240.
(8) Rotenberg, N.; Kuipers, L. Mapping Nanoscale Light Fields. *Nat. Photonics* **2014**, *8* (12), 919−926.
(9) Kasperczyk, M.; Person, S.; Ananias, D.; Carlos, L. D.; Novotny, L. Excitation of Magnetic Dipole Transitions at Optical Frequencies. *Phys. Rev. Lett.* **2015**, *114* (16), 163903.
(10) Zhou, J.; Koschny, T.; Kafesaki, M.; Economou, E. N.; Pendry, J. B.; Soukoulis, C. M. Saturation of the Magnetic Response of Split-Ring Resonators at Optical Frequencies. *Phys. Rev. Lett.* **2005**, *95* (22), 223902.
(11) Banzer, P.; Peschel, U.; Quabis, S.; Leuchs, G. On the Experimental Investigation of the Electric and Magnetic Response of a Single Nano-Structure. *Opt. Express* **2010**, *18* (10), 10905.
(12) Vaskin, A.; Mashhadi, S.; Steinert, M.; Chong, K. E.; Keene, D.; Nanz, S.; Abass, A.; Rusak, E.; Choi, D.-Y.; Fernandez-Corbaton, I.; et al. Manipulation of Magnetic Dipole Emission from Eu 3+ with Mie-Resonant Dielectric Metasurfaces. *Nano Lett.* **2019**, *19* (2), 1015−1022.
(13) Aigouy, L.; Cazé, A.; Gredin, P.; Mortier, M.; Carminati, R. Mapping and Quantifying Electric and Magnetic Dipole Luminescence at the Nanoscale. *Phys. Rev. Lett.* **2014**, *113* (7), 076101.
(14) Shafiei, F.; Monticone, F.; Le, K. Q.; Liu, X.-X.; Hartsfield, T.; Alù, A.; Li, X. A Subwavelength Plasmonic Metamolecule Exhibiting Magnetic-Based Optical Fano Resonance. *Nat. Nanotechnol.* **2013**, *8* (2), 95−99.
(15) Meng, Y.; Zhang, Q.; Lei, D.; Li, Y.; Li, S.; Liu, Z.; Xie, W.; Leung, C. W. Plasmon-Induced Optical Magnetism in an Ultrathin Metal Nanosphere-Based Dimer-on-Film Nanocavity. *Laser Photonics Rev.* **2020**, *14* (9), 2000068.
(16) Rabouw, F. T.; Prins, P. T.; Norris, D. J. Europium-Doped NaYF4 Nanocrystals as Probes for the Electric and Magnetic Local Density of Optical States throughout the Visible Spectral Range. *Nano Lett.* **2016**, *16* (11), 7254−7260.
(17) le Feber, B.; Sipe, J. E.; Wulf, M.; Kuipers, L.; Rotenberg, N. A Full Vectorial Mapping of Nanophotonic Light Fields. *Light: Sci. Appl.* **2019**, *8* (1), 28.
(18) Davis, T. J.; Janoschka, D.; Dreher, P.; Frank, B.; Meyer zu Heringdorf, F.-J.; Giessen, H. Ultrafast Vector Imaging of Plasmonic Skyrmion Dynamics with Deep Subwavelength Resolution. *Science* **2020**, *368* (6489), eaba6415.
(19) Meng, F.; Yang, A.; Shi, P.; Du, L.; Yuan, X. Mapping the Near-Field Distribution of Magnetic Fields Using a Silicon Nanoparticle at Optical Frequencies. *J. Phys. D: Appl. Phys.* **2019**, *52* (35), 355002.
(20) Neugebauer, M.; Eismann, J. S.; Bauer, T.; Banzer, P. Magnetic and Electric Transverse Spin Density of Spatially Confined Light. *Phys. Rev. X* **2018**, *8* (2), 021042.
(21) Kuznetsov, A. I.; Miroshnichenko, A. E.; Fu, Y. H.; Zhang, J.; Luk'yanchuk, B. Magnetic Light. *Sci. Rep.* **2012**, *2* (1), 492.
(22) Shcherbakov, M. R.; Neshev, D. N.; Hopkins, B.; Shorokhov, A. S.; Staude, I.; Melik-Gaykazyan, E. V.; Decker, M.; Ezhov, A. A.; Miroshnichenko, A. E.; Brener, I.; et al. Enhanced Third-Harmonic Generation in Silicon Nanoparticles Driven by Magnetic Response. *Nano Lett.* **2014**, *14* (11), 6488−6492.
(23) Smirnova, D.; Kivshar, Y. S. Multipolar Nonlinear Nanophotonics. *Optica* **2016**, *3* (11), 1241.
(24) Zhang, C.; Xu, Y.; Liu, J.; Li, J.; Xiang, J.; Li, H.; Li, J.; Dai, Q.; Lan, S.; Miroshnichenko, A. E. Lighting up Silicon Nanoparticles with Mie Resonances. *Nat. Commun.* **2018**, *9* (1), 2964.
(25) Xiang, J.; Chen, J.; Dai, Q.; Tie, S.; Lan, S.; Miroshnichenko, A. E. Modifying Mie Resonances and Carrier Dynamics of Silicon Nanoparticles by Dense Electron-Hole Plasmas. *Phys. Rev. Appl.* **2020**, *13* (1), 014003.
(26) Novotny, L.; Beversluis, M. R.; Youngworth, K. S.; Brown, T. G. Longitudinal Field Modes Probed by Single Molecules. *Phys. Rev. Lett.* **2001**, *86* (23), 5251−5254.
(27) Baranov, D. G.; Savelev, R. S.; Li, S. V.; Krasnok, A. E.; Alù, A. Modifying Magnetic Dipole Spontaneous Emission with Nanophotonic Structures. *Laser Photon. Rev.* **2017**, *11* (3), 1600268.
(28) Evlyukhin, A. B.; Fischer, T.; Reinhardt, C.; Chichkov, B. N. Optical Theorem and Multipole Scattering of Light by Arbitrarily Shaped Nanoparticles. *Phys. Rev. B: Condens. Matter Mater. Phys.* **2016**, *94* (20), 205434.
(29) Alaee, R.; Rockstuhl, C.; Fernandez-Corbaton, I. An Electromagnetic Multipole Expansion beyond the Long-Wavelength Approximation. *Opt. Commun.* **2018**, *407*, 17−21.
(30) Ghenuche, P.; Cherukulappurath, S.; Taminiau, T. H.; van Hulst, N. F.; Quidant, R. Spectroscopic Mode Mapping of Resonant Plasmon Nanoantennas. *Phys. Rev. Lett.* **2008**, *101* (11), 116805.
(31) Beversluis, M.; Bouhelier, A.; Novotny, L. Continuum Generation from Single Gold Nanostructures through Near-Field Mediated Intraband Transitions. *Phys. Rev. B: Condens. Matter Mater. Phys.* **2003**, *68* (11), 115433.
(32) Novotny, L.; Hecht, B. *Principles of Nano-Optics*, 2nd ed.; Cambridge University Press: New York, 2012.
(33) Makarov, S. V.; Petrov, M. I.; Zywietz, U.; Milichko, V.; Zuev, D.; Lopanitsyna, N.; Kuksin, A.; Mukhin, I.; Zograf, G.; Ubyivovk, E.; et al. Efficient Second-Harmonic Generation in Nanocrystalline Silicon Nanoparticles. *Nano Lett.* **2017**, *17* (5), 3047−3053.
(34) Cazzanelli, M.; Schilling, J. Second Order Optical Nonlinearity in Silicon by Symmetry Breaking. *Appl. Phys. Rev.* **2016**, *3* (1), 011104.
(35) Sun, L.; Bai, B.; Meng, X.; Cui, T.; Shang, G.; Wang, J. Near-Field Probing the Magnetic Field Vector of Visible Light with a Silicon Nanoparticle Probe and Nanopolarimetry. *Opt. Express* **2018**, *26* (19), 24637.
(36) Feng, T.; Xu, Y.; Zhang, W.; Miroshnichenko, A. E. Ideal Magnetic Dipole Scattering. *Phys. Rev. Lett.* **2017**, *118* (17), 173901.
(37) Baranov, D. G.; Zuev, D. A.; Lepeshov, S. I.; Kotov, O. V.; Krasnok, A. E.; Evlyukhin, A. B.; Chichkov, B. N. All-Dielectric Nanophotonics: The Quest for Better Materials and Fabrication Techniques. *Optica* **2017**, *4* (7), 814.
(38) Haug, T.; Klemm, P.; Bange, S.; Lupton, J. M. Hot-Electron Intraband Luminescence from Single Hot Spots in Noble-Metal Nanoparticle Films. *Phys. Rev. Lett.* **2015**, *115* (6), 067403.
(39) Palik, E. D. *Handbook of Optical Constants of Solids*, 1st ed.; Elsevier Ltd.: Oxford, 2012.

■ NOTE ADDED AFTER ASAP PUBLICATION

This paper was published ASAP on March 2, 2021, with the incorrect version of the Supporting Information. The corrected version was reposted on March 4, 2021.

https://dx.doi.org/10.1021/acs.nanolett.0c04706
Nano Lett. 2021, 21, 2453−2460